

## Finding a Crack and Determining Depth in a Material

**Abstract.** The purpose of this paper is to find geometry of a crack (length and depth) in a conductive plate, on the basis of non-destructive testing with eddy currents. The position of a crack can be determined by taking into consideration the change in the magnetic density between the measured points. The depth is determined with the use of FEM model. The calculated test case points to an accurate determination.

**Streszczenie.** W artykule opisano metodę wyznaczania rozmiarów pęknięć w płytkach przewodzących, na podstawie testów z wykorzystaniem prądów wirowych, nieniszczących elementu. Metoda wykorzystuje wpływ pęknięć na zmianę gęstości pola w badanym rejonie. W analizie posłużono się metodą elementów skończonych. Otrzymane wyniki potwierdzają skuteczność działania. (Lokalizacja i analiza rozmiarów pęknięć w materiale przewodzącym).

**Keywords:** Measurements, finite element method, non-destructive testing.

**Słowa kluczowe:** pomiary, metoda elementów skończonych, próba nieniszcząca.

### Introduction

The method of identifying and searching for a crack, with a non-destructive testing, is all more widespread and important [1,2,3,4]. Non-destructive testing is often used, based on considering the impact of eddy currents and the usage of different excitation coils and sensors for measuring magnetic flux density [5,6,7].

Several devices for non-destructive testing have additional programs for displaying measurement results, within which a graphical display of the measured results helps to determine the position of a crack within a material [8].

This paper describes a procedure that determines a crack's position on the basis of measurements. The input data is represented by the measured values for magnetic flux density at the centre of an excitation coil, supplied with an alternating current. Our intention was to also determine a crack's depth. This meant dealing with an inverse problem. Some authors use analytical methods that help to solve the problem [9,10,11].

Sometimes numerical methods are used to achieve better results, which are further used to analyse certain circumstances within those tested materials close to the excitation coils [12].

Our strategy is based over two steps. Firstly, calculation of the crack's length using the derivatives at each measured point towards the neighbouring measuring points. Secondly, the determination of crack depth using a FEM model, combined with an iterative procedure.

A program that defines a position and depth of a crack, in a material, is developed and presented in the paper.

### Measurements

The basis for geometry of a test case is geometry of the Team Workshop problem No. 8.

The test case is an aluminium plate with a crack, above which is an excitation coil. Plate with a crack and coil with marked dimensions are shown in Figure 1.

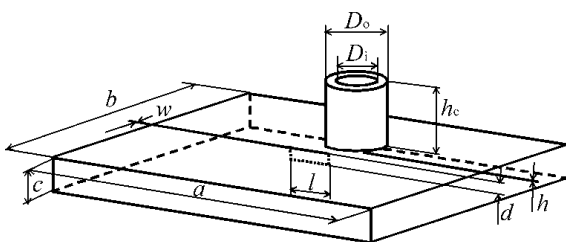


Fig. 1. Plate with crack and coil.

Plate thickness is  $c = 30$  mm and dimensions  $a = 330$  mm and  $b = 285$  mm. The crack is in the middle of a plate. The position of a crack is determined with the help of a coil, which is placed at  $h = 7.8$  mm above the plate. The coil has 566 turns, inner diameter  $D_i = 36.8$  mm, outside diameter  $D_o = 53$  mm and height  $h_c = 56$  mm. The coil is supplied with a sinusoidal current of 1 A and frequency of 500 Hz. The crack has a depth  $d = 10$  mm, length  $l = 40$  mm and width  $w = 0.5$  mm. The measuring is only conducted with a z component (magnitude) of magnetic flux density in an axle of the coil at 0.5 mm above the plate.

Values obtained through measurements are shown in Figure 2.

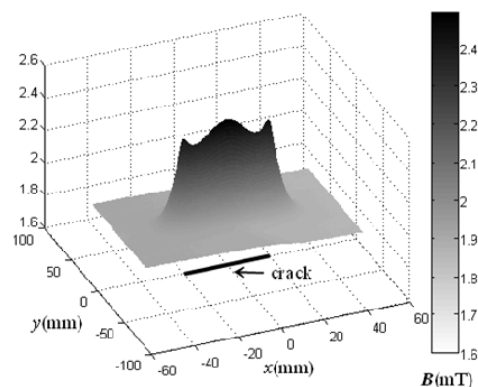


Fig. 2. Measured values above the crack size  $d = 10$  mm and  $w = 0.5$  mm.

### Determining a crack position and length

The measured  $B_z$  are exemplified with surface, whose shape is dependent from crack parameters (length, depth and width).

The lower eddy current occur in the area of the crack, therefore the density of magnetic flux increases.

Study of influence of depth and width of crack on magnetic density over the plate is made with use of finite element method (FEM) model. Cedrat Flux 3D software is used for simulations. Model for simulations is shown in Figure 3.

Absolute value of magnetic density z-component, above the plate, has a shape of the surface that is shown in Figure 4. The shape of a surface changes in relation to changes of length, width and depth of a crack. Presented in the Figure 4 is a left half of the picture (from  $y = 0$  to  $y = 10$  mm) where

length of a crack is 40 mm, width of a crack is 0.5 mm and depth of a crack is 10 mm, as well as the right half of the picture (from  $y = -10$  mm to  $y = 0$ ) where length of a crack is 40 mm, width of a crack is 0.5 mm and depth of a crack is 5 mm.

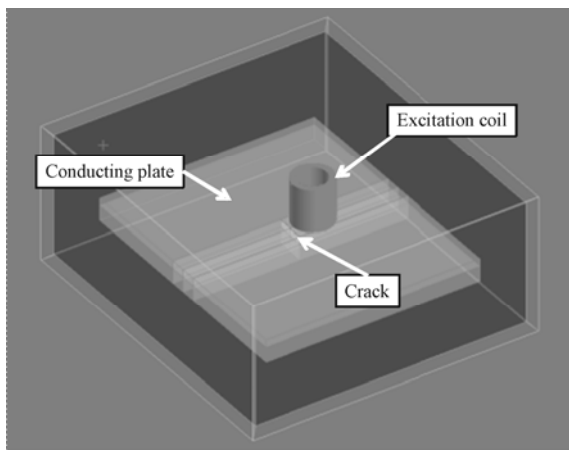


Fig.3. Flux 3D model for simulations

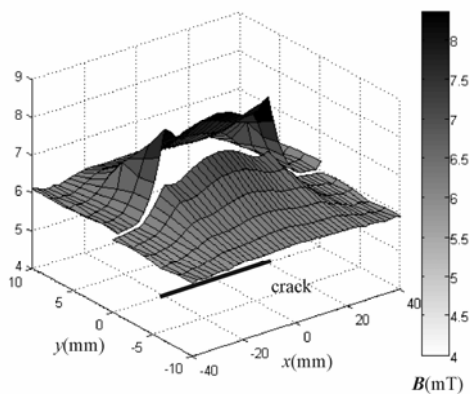


Fig.4.  $B_z$  for different positions of coil - length of crack 40 mm, width of crack 0.5 mm, depth of crack 5 mm ( $-10 \text{ mm} \leq y \leq 0$ ) and 10 mm ( $0 \leq y \leq 10 \text{ mm}$ )

That way the crack position is determined by considering the change in density – derivatives on the plane in measured points. In every measured point, the derivatives are calculated in the direction of neighbouring measured points, and there are eight directions.

The derivatives are calculated as differential quotients, which are expressed as angles. The angles are obtained through an Equation (1).

$$(1) \quad \varphi_i = \tan^{-1} \left( \frac{B_i - B_c}{\sqrt{(x_i - x_c)^2 + (y_i - y_c)^2}} \right)$$

Obtained angles can be 0, positive or negative. If the magnetic density in neighbouring measured point does not change, then the angle equals 0. If it increased then the angle is positive and if it decreased the angle is negative. Directions of derivatives within some points are shown in Figure 5.

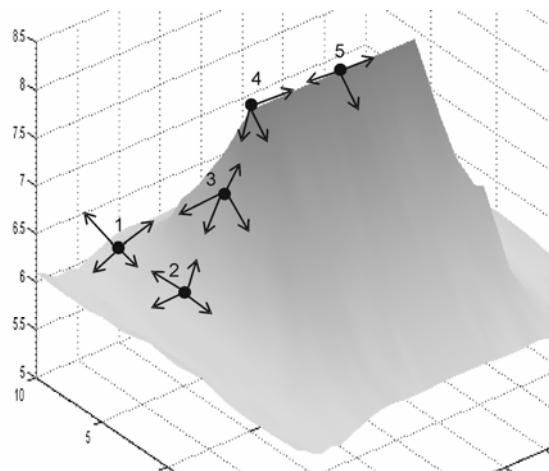


Fig.5. Directions of derivatives in some points

For every point, there are eight derivative values in the direction of eight neighbouring measured points. Due to clarity in Figure 5, not all derivative directions into an individual point are shown.

In order to determine a crack, it is sufficient enough to know the maximum and minimum angle respectively derivative of the magnetic field density.

The minimum and maximum angles are presented in Figure 6.

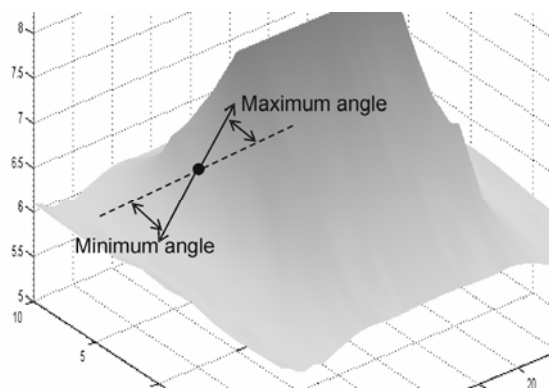


Fig.6. Minimum and maximum angle

The crack in the material occurs when the minimum angle is smaller than zero and maximum angle approximately equal to zero (points 4 and 5 in Figure 5 and in Table 1) or when the minimum angle is smaller than zero and maximum angle is smaller than zero. During the calculation, a certain tolerance (value smaller than tolerance is considered as 0 – tolerance is between 1 and 2 degrees) is taken into consideration since the plane of the measured values is not completely smooth.

Table 1. Determining a crack in points in Figure 5 depending on  $\varphi_{\min}$  and  $\varphi_{\max}$

Point	1	2	3	4	5
$\varphi_{\min}$	$\approx 0$	$\approx 0$	$< 0$	$< 0$	$< 0$
$\varphi_{\max}$	$\approx 0$	$> 0$	$> 0$	$\approx 0$	$\approx 0$
Crack	No	No	No	Yes	Yes

Results obtained for the test example are shown in the Figure 7.

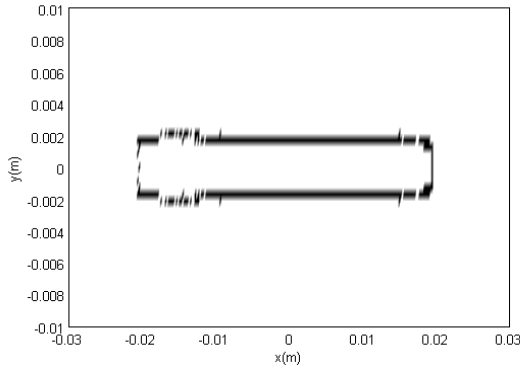


Fig.7. Determined position of a crack

Based on a condition that  $\varphi_{\min} < 0$  and  $\varphi_{\max} \approx 0$  or  $\varphi_{\min} < 0$  and  $\varphi_{\max} < 0$  the course of a crack is correctly determined. The obtained length of the crack in the Figure 7 is 39.4 mm, which is correct value. The obtained width of the crack in the Figure 7 is 3.4 mm, which is not the width of a real crack. In order to obtain the approximately correct crack width, the measured  $B_z$  should have started to decrease on the border of the crack, but it started to decrease some measured points away from the crack's border.

Based on a determined position of a crack, the FEM model is made with an appropriate mesh of finite elements. The mesh is denser around the crack, while the areas away from the crack may have increased number of finite elements. In the area of the crack and partially near the crack, a mesh is made in layers that are parallel with a crack. That way the thickness of a mesh can be easily changed by moving the layer knots in FEM model where another generation of FEM mesh is not necessary. Finite elements in the shape of a prism are used, of which the basic plains lie in a flat surface parallel with a plain of the plate. In such way, with the change of the z-coordinate of an individual surface in the finite element mesh, the depth of a crack can be changed. Shown in Figure 8 is a schematic display of the way the finite element mesh, in the area of the crack, is generated. In case it comes to large changes of  $d$  and  $w$ , the surrounding layers of finite element mesh are adjusted around the z and y axle.

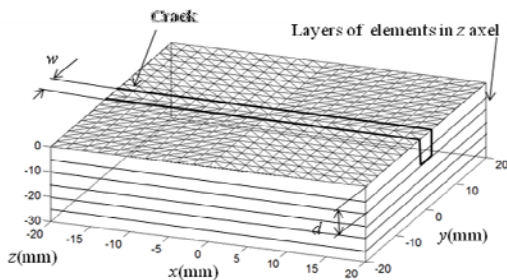


Fig.8. Schematic display of the way the finite elements mesh is generated

### Determining depth of a crack

Depth ( $d$ ) and width ( $w$ ) influence the course of density. The course of density above the crack can be more or less curved. The difference is mainly above and in the vicinity of a crack. The knowledge of this course, which is obtained from the measurement, makes it possible to determine depth  $d$ .

A program has been developed that connects Finite elements model with an iterative method, which makes it

possible to detect a crack. The  $\mathbf{A} - V$ ,  $\mathbf{A}$  formulation is utilized where in a conducting region, a magnetic vector potential  $\mathbf{A}$  and electric scalar potential  $V$  are used and in non-conducting region, only the magnetic vector potential  $\mathbf{A}$  is used [9].

Complex equations are used due to a harmonic excitation of current and the linear features of a material.

Differential equations (2) and (3) are solved in conductive region.

$$(2) \quad \text{rot} \left( \frac{1}{\mu} \text{rot} \mathbf{A} \right) + j\omega\sigma\mathbf{A} + \sigma \text{grad} V = 0$$

$$(3) \quad \text{div} (j\omega\sigma\mathbf{A} + \sigma \text{grad} V) = 0$$

Differential equation (4) is solved in non-conducting area.

$$(4) \quad \text{rot} \left( \frac{1}{\mu} \text{rot} \mathbf{A} \right) = J_e$$

$J_e$  is excitation current. Eddy currents are not considered in an area of the coil.

That way the system is solved, where coefficients are complex numbers written with a matrix equation (5).

$$(5) \quad [\mathbf{S}] \cdot [\mathbf{P}] = [\mathbf{R}]$$

$\mathbf{S}$  is a system matrix that is dependant on the geometry and material properties,  $\mathbf{P}$  is a vector of potentials and  $\mathbf{R}$  is a vector of excitation.

In relationship to the geometry of a crack, the FEM calculation is conducted for every iteration of an algorithm, only in few typical points. The points are chosen from the top and next to a crack, in a transverse direction in relation to the crack. If the crack is uniform, it is enough to choose only those points transversely in the middle of the crack. If not, the points on the greater number of lines, transversely to the crack, must be chosen. As a result, an average value of depth of a crack is obtained.

Appropriate choice of number of points considerably shortens the calculation time and does not impact on the accuracy of the calculation.

Width is set as a constant value and depth is calculated on the basis of typical points (for the test case we used nine points). The calculation of the new depth for each point is made with Equation (6). Use of Equation (6) leads us iteratively to the solution.

$$(6) \quad d_i^{(k)} = d_i^{(k-1)} - \frac{(d_i^{(k-1)} - d_i^{(k-2)}) \cdot (B_i^{(k-1)} - B_{mi})}{(B_i^{(k-1)} - B_{mi}) - (B_i^{(k-2)} - B_{mi})}$$

And new depth is calculated with Equation (7).

$$(7) \quad d^{(k)} = \frac{\sum_{i=1}^n d_i^{(k)}}{n}$$

$B_i$  are calculated values in individual point,  $B_{mi}$  measured values in individual point and  $n$  is number of chosen typical points. The calculation is made for three different crack widths and the sum of squares of differences between measured and calculated values is calculated with Equation (8).

$$(8) \quad sum = \frac{\sqrt{\sum_{i=1}^n (B_i - B_{mi})^2}}{n}$$

The entire calculation procedure is shown through an algorithm in Figure 9.

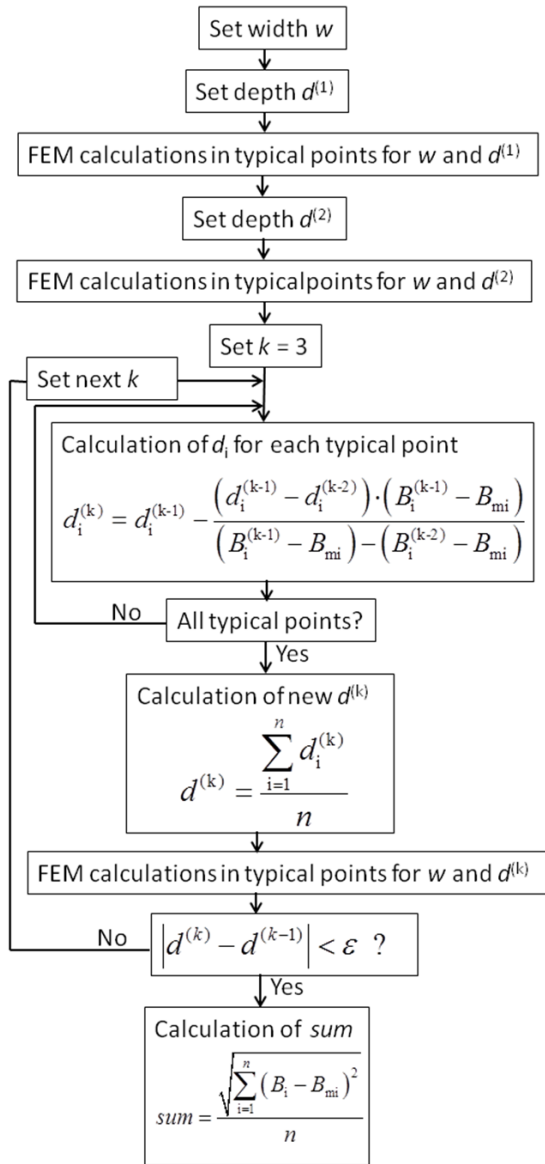


Fig.9. Calculation algorithm

$k$  is the iteration number and  $\varepsilon$  is the difference between the two calculated depths, which must be reached.

### Results

Test calculation was made for three different crack widths, which were 0.5, 1 and 1.5 mm. The iterative procedure was made until the difference between the two calculated values of  $d$  was smaller than  $10^{-6}$  m.

Calculation results are presented in the Table 2.

Table 2. Calculated depth for different widths

$w$ (mm)	$d$ (mm)	iterations	sum
0.5	7.1995	26	$1.22812 \cdot 10^{-5}$
1	8.7529	13	$7.826 \cdot 10^{-6}$
1.5	8.6522	12	$1.229654 \cdot 10^{-5}$

On the basis of results from Table 2, it can be seen that the  $sum$  is the smallest, for the crack width 1 mm. It can be concluded that the crack depth is 8.75 mm. For more exact solution, more calculations for crack widths around 1 mm should be done. On computers, which have processors with multiple cores, the calculations for different widths can be done parallel (as separate exe files or as parallel processing).

### Conclusions

The length of the found crack is 39.4 mm. That is correct solution. The found depth is 8.75 mm, which deviates 12.5% from the actual depth of 10 mm. The problem is poorly conditional in a sense of a search of the crack width: therefore the crack width of 1 mm is only estimation. To get more exact value, further calculations with different crack widths must be conducted. In that case the calculated crack depth will remain almost the same. Very thin crack lead us to the very small finite elements in the crack area, which is not possible to model.

### REFERENCES

- [1] Vasić D., Bilas V., Šnajder B., Analytical modeling in low-frequency electromagnetic measurements of steel casing properties, *NDT&E International*, 40 (2007), 103-111
- [2] Yuso N., Perrin S., Mizuno K., Miya K., Numerical modeling of general cracks from the viewpoint of eddy current simulations, *NDT&E International*, 40 (2007), 577-583
- [3] Zeng Z., Udpa L., Udpa S., Finite-Element Model for Simulations of Ferrite-Core Eddy Current-Probe, *IEEE Trans. Magn.*, 46 (2010), No. 3, 905-909
- [4] Zeng Z., Udpa L., Udpa S., Chan M., Reduced Magnetic Vector Potential Formulation in the Finite Element Analysis of Eddy Current Nondestructive Testing, *IEEE Trans. Magn.*, 45 (2009), No. 3, 964-967
- [5] Gilles-Pascaud C., Pierantoni M., Eddy current array probe development for non-destructive testing, *16<sup>th</sup> World Conference on NDT, 30 August – 3 September, Montreal, Canada, 2004*
- [6] Tian G., Sophian A., Study of Magnetic sensors for pulsed eddy current techniques, *16<sup>th</sup> World Conference on NDT, 30 August – 3 September, Montreal, Canada, 2004*
- [7] Fava J., Obrutsky A., Ruch M., Design and construction of eddy current sensors with rectangular plane coils, *16<sup>th</sup> World Conference on NDT, 30 August – 3 September, Montreal, Canada, 2004*
- [8] Pichenot G., Buvat F., Maillot V., Voillaume H., Eddy current modelling for non-destructive testing, *16<sup>th</sup> World Conference on NDT, 30 August – 3 September, Montreal, Canada, 2004*
- [9] Preis K., Biro O., Magele C., Renhard W., Richter K.R., Vrisk G., Numerical Analysis of 3D Magnetostatic Fields, *IEEE Trans. Magn.*, 27 (1991), No. 5, 3798-3803

**Authors:** assistant prof. dr. Marko Jesenik, University of Maribor, Faculty of Electrical Engineering and Computer Science, Smetanova ul. 17, 2000 Maribor, Slovenia, E-mail: [jesenik@uni-mb.si](mailto:jesenik@uni-mb.si), full prof. dr. Mladen Trlep, University of Maribor, Faculty of Electrical Engineering and Computer Science, Smetanova ul. 17, 2000 Maribor, Slovenia, E-mail: [mladen.trlep@uni-mb.si](mailto:mladen.trlep@uni-mb.si)